



Since January 2020 Elsevier has created a COVID-19 resource centre with free information in English and Mandarin on the novel coronavirus COVID-19. The COVID-19 resource centre is hosted on Elsevier Connect, the company's public news and information website.

Elsevier hereby grants permission to make all its COVID-19-related research that is available on the COVID-19 resource centre - including this research content - immediately available in PubMed Central and other publicly funded repositories, such as the WHO COVID database with rights for unrestricted research re-use and analyses in any form or by any means with acknowledgement of the original source. These permissions are granted for free by Elsevier for as long as the COVID-19 resource centre remains active.



## Short communication

# Surface plasmon resonance approach to study drug interactions with SARS-CoV-2 RNA-dependent RNA polymerase highlights treatment potential of suramin

Martina Mravinec, Gregor Bajc, Matej Butala \*

Department of Biology, Biotechnical Faculty, University of Ljubljana, Ljubljana 1000, Slovenia



## ARTICLE INFO

## Keywords:

SARS-CoV-2  
RNA-dependent RNA polymerase  
Surface plasmon resonance  
Suramin

## ABSTRACT

The SARS-CoV-2 RNA-dependent RNA polymerase (RdRp) is essential for virus replication, therefore it is a promising drug target. Here we present a surface plasmon resonance approach to study the interaction of RdRp with drugs in real time. We monitored the effect of favipiravir, ribavirin, sofosbuvir triphosphate PSI-7409 and suramin on RdRp binding to RNA immobilized on the chip. Suramin precluded interaction of RdRp with RNA and even displaced RdRp from RNA.

The SARS-CoV-2 pandemic has changed the world as we know it. With no less than 140 million people infected and over 3 million deaths, it has become a focal point for researchers around the world looking into the nature of the virus and, more importantly, the cure. RNA polymerase is a promising drug target because its inhibition prevents the virus from replicating in living cells. It is also evolutionarily very stable compared to surface proteins (Shi et al., 2013). SARS-CoV-2 nonstructural proteins (nsps) encoded by the first two open reading frames (ORF1ab) constitute the replication and transcription complex that controls the virus life cycle (Wu et al., 2020; Ziebuhr, 2005). The nsp12 is the catalytic subunit of the RNA-dependent RNA polymerase (RdRp) (Ahn et al., 2012), which is capable of basal polymerase activity, but when bound to the cofactors nsp7 and nsp8, the efficiency of polymerase activity increases significantly (Subissi et al., 2014; Zhai et al., 2005). Promising inhibitors targeting the polymerase are nucleotide analogues (Ju et al., 2020; Öberg, 2006), e.g. remdesivir, which has shown great success in inhibiting viral polymerase and specifically SARS-CoV-2 RdRp (Agostini et al., 2018; Gordon et al., 2020; Kokic et al., 2021). Sofosbuvir, a uridine nucleoside analogue (Jácome et al., 2020; Jockusch et al., 2020), ribavirin, a guanoside nucleoside analogue (Elfiky, 2020), favipiravir, a purine analogue (Abdelnabi et al., 2017; Furuta et al., 2005), and the 100-year-old drug suramin (Salgado-Benvindo et al., 2020; Wiedemar et al., 2020; Yin et al., 2021) also have great potential.

Here we report an efficient surface plasmon resonance (SPR) approach for screening drugs targeting SARS-CoV-2 RdRp (nsp12-nsp7-nsp8). We performed SPR analysis at 25 °C on the Biacore T200 system

using a streptavidin-coated SPR biosensor chip (SA chip, GE Healthcare). Interaction measurements were performed in running buffer 45 mM Tris-HCl, 140 mM NaCl, 2.5 mM KCl, 4 mM MgCl<sub>2</sub>, 0.005 % Tween 20, pH 8. First, a biotinylated, 15 nt oligonucleotide (5'-CGCTCGAGTAGTAAC-Bio-3') with 30 response units (RU) was immobilized on the surface of flow cells (Fc) 1 and 2 of the SA chip (Formelos et al., 2015). Next, we designed the RNA molecule to hybridize to the oligonucleotide and enable the interaction with RdRp (Fig. 1A). For this purpose, we used RNA that self-anneals at the 3'-end into the U-tetraloop and was used to resolve the SARS-CoV-2 RdRp structure in complex with RNA (Hillen et al., 2020), flanked by 26 nucleotides, carrying at the 5'-end the sequence complementary to the chip-immobilized oligonucleotide (5'-GUUACUACUCGAGCGUUUUCAUCAUUCGCGUAGUUUCUACGCG-3', SigmaAldrich). To initiate proper folding and annealing, RNA was diluted in buffer 10 mM Tris, 50 mM NaCl, 1 mM EDTA, pH 8 at a concentration of 50 μM and annealed in Thermo Cycler by heating RNA to 75 °C for 5 min and then gradually cooling to 4 °C (temperature drop of 5 °C every 3 min). Annealed RNA at a concentration of 2 μM, was injected over Fc2 (flow rate 5 μL/min, association time 200 s) to 45 RU.

To assay the interaction of SARS-CoV-2 RdRp (nsp12-nsp7-nsp8 complex, BPS Bioscience #100839) with RNA immobilized on the chip, we performed the single cycle kinetics experiment. For this purpose, we injected RdRp (2.5, 5, 10, 20, 40 nM) from the low to the high concentration across the Fc1 and Fc2 at a flow rate of 30 μL/min, association time 120 s, with short dissociation times in between and a dissociation step of 200 s at the end. The sensorgrams show concentration-dependent

\* Corresponding author at: Department of Biology, Biotechnical Faculty, University of Ljubljana, Večna pot 111, Ljubljana, Slovenia.  
E-mail address: [matej.butala@bf.uni-lj.si](mailto:matej.butala@bf.uni-lj.si) (M. Butala).

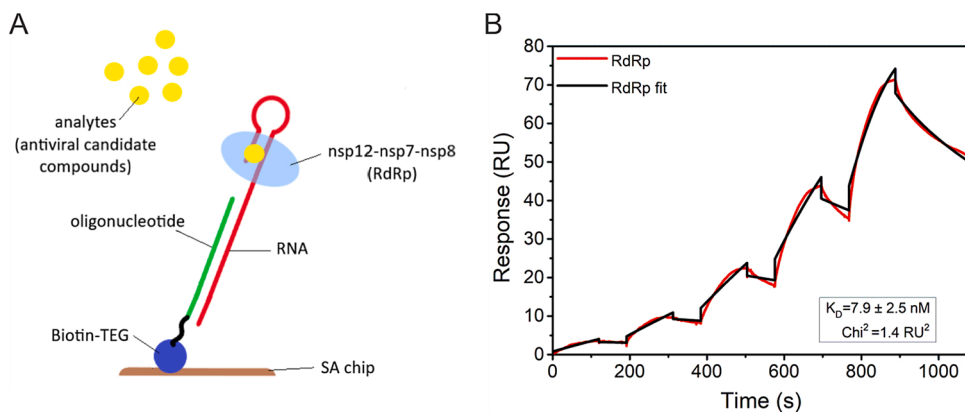


**Fig. 1.** Interaction of RNA dependent RNA polymerase with chip-immobilized RNA. (A) Schematic representation of SA chip surface encompassing biotin-tetraethylene glycol (TEG) oligonucleotide (green), RNA with U-tetra loop (red) hybridized to the biotinylated oligonucleotide, RdRp interacting with RNA (blue), and its analytes (antiviral candidate compounds, yellow) used to monitor interactions. (B) Surface plasmon resonance analysis of RdRp binding to immobilized RNA (2  $\mu$ M) on SA chip using a single cycle kinetics approach via consecutive injections of RdRp at concentrations of 2.5, 5, 10, 20, and 40 nM (from left to right) (red). The equilibrium constant ( $K_D$ ) of  $7.9 \pm 2.5$  nM was calculated from three experiments. Sensorgram fitting was performed using Biacore T-200 Evaluation Software, 1:1 binding kinetics model (black).

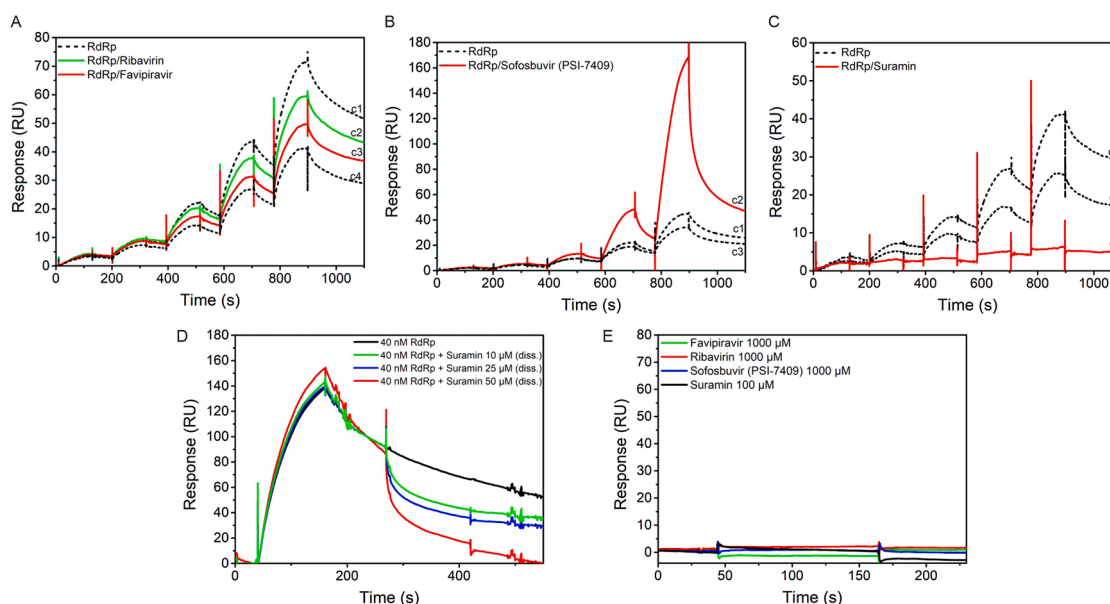


**Fig. 2.** SPR analysis of the effect of potential inhibitors on the binding of RdRp to immobilized RNA. (A-C) SPR sensorgrams of RdRp (2.5, 5, 10, 20, and 40 nM, consecutive injections at a flow rate of 30  $\mu$ L/min, association time 120 s), either alone (black sensorgrams, dashed lines) or mixed with selected compound with the RNA immobilized on the SA chip. Note that in panels A-C only RdRp was injected over the RNA before (upper black sensorgram, cycle 1, c1) and after (lower black sensorgram) RdRp mixed with selected compound was injected to exclude the effect of decreased RdRp-RNA binding during the course of the experiment. The first analysis cycle is labelled c1 and subsequent cycles of compound/RdRp injections are labelled c2, c3, c4. (A) Sensorgrams of RdRp in the presence of either ribavirin (green) or favipiravir (red), at a molar ratio of RdRp to compound 1:25000, showing that these two compounds do not affect RdRp-RNA interaction. (B) Sensorgram of injections of RdRp together with PSI-7409 (1:25000, mol:mol) (red), showing an increased response of binding to RNA compared to free RdRp (dashed black lines). (C) Sensorgram of RdRp mixed with suramin at a molar ratio of 1:2500 (red) shows that suramin inhibits the interaction of RdRp with RNA immobilized on the chip. (D) RdRp (40 nM) was injected over the chip-immobilized RNA for 100 s at 30  $\mu$ L/min. Subsequently, in the dissociation phase, suramin at a concentration of 10, 25 or 50  $\mu$ M was injected over the nucleoprotein complex at time 280 s for 150 s and dissociation was followed for 60 s. Suramin displaced RdRp from RNA in a concentration-dependent manner, with 50  $\mu$ M suramin displacing most of RdRp (red). Sensorgrams were normalized on the Y axis to 100 response units of RdRp in the dissociation phase when the suramin was injected (Biacore T-200 Evaluation Software). Experiments were performed in duplicates and representative sensorgrams are shown. (E) Interaction of the studied compounds, at the highest concentrations used in the experiments, the results of which are shown in panels A-D, with immobilised RNA.

RdRp binding with the RNA immobilized on the chip, exhibiting an apparent equilibrium constant ( $K_D$ ) of  $\sim 7.9 \pm 2.5$  nM (Fig. 1B) and maximum response of 75 RU. We observed that fewer response units of RdRp associated with RNA over the course of the experiment, as the maximum response of RdRp binding to RNA decreased by approximately 20 RU per 60 min. We believe that the reason for this is most likely due to unwinding of the RNA U-tetra loop in a part of the chip-immobilized RNA molecules. Nevertheless, by injecting free RdRp at the beginning and at the end of each measurement as a control, we were able to examine the effect of selected compounds on RdRp-RNA

interaction. We analyzed the effects of ribavirin, favipiravir, and suramin in their nonmetabolite forms and sofosbuvir in its active triphosphate metabolite form, called PSI-7409. All compounds were purchased from MedChemExpress (Ribavirin #HY-B0434, Favipiravir #HY-14768, PSI-7409 #HY-15745, Suramin sodium salt #HY-B0879A).

RdRp was mixed with each inhibitor at the desired ratio and injected over the RNA immobilized on the SA chip (the same single cycle kinetics experiment as described above was used). It is worth noting that in all experiments the sensorgrams were referenced twice, for the response of the untreated surface of the flow cell 1 with solely immobilized

biotinylated oligo and the response of the buffer. The sensor surface was regenerated by a 8-second injection of 50 mM NaOH, resulting in dissociation of the RNA-RdRp complex. After the regeneration step, 45 RU of RNA was immobilized on the test flow cell 2. Ribavirin and favipiravir, both in the ratio to RdRp 25000:1 (mol:mol), showed no significant effect on the binding of RdRp to RNA (Fig. 2A). This is as expected, since these nucleoside analogs only interact with RdRp when metabolized to their triphosphate forms in the cell (Agostini et al., 2018; Furuta et al., 2005; Tchesnokov et al., 2019). Sofosbuvir has already shown major inhibitory effects on Zika virus (Reznik and Ashby, 2017), as well as on SARS-CoV-2 (Chien et al., 2020; Jácome et al., 2020; Jockusch et al., 2020; Ju et al., 2020). In its triphosphate form, it binds to RdRp, which it mistakes for a nucleotide and inserts into emerging RNA chain. This leads to termination of RNA polymerization, resulting in viral decay (Jockusch et al., 2020). We measured a higher RdRp response when mixed with PSI-7409 (PSI-7409 : RdRp, 25000:1, mol:mol). The difference in response between free RdRp and RdRp mixed with PSI-7409 is most noticeable at higher concentrations (highest response is 170 RU). We observe that this drug does not prevent RdRp from binding to RNA and it does not bind to RNA itself. We speculate that the observed response may be due to PSI-7409 enhancing the affinity of RdRp for nucleic acids immobilized on the chip or/and due to the nonspecific binding of PSI-7409 to RdRp (Fig. 2B).

RdRp mixed with suramin at a molar ratio of 1:2500 lost its ability to bind to RNA immobilized on the chip (Fig. 2C). This is consistent with previous experiments showing that suramin inhibits viral replication by binding to RdRp, thus eliciting site clashes with the RNA strand near the catalytic active site of RdRp and directly blocking the binding of the RNA template strand (Yin et al., 2021). To further demonstrate that suramin has the ability to interfere with RdRp-RNA binding, we injected 40 nM RdRp (flow rate 30  $\mu$ L/min, association time 100 s) over the RNA immobilized on the chip (45 RU) and followed the dissociation of the nucleoprotein complex. The data show that subsequent injection of suramin in 10  $\mu$ M or 25  $\mu$ M or 50  $\mu$ M displaces RdRp from the RNA in a concentration-dependent manner (Fig. 2D). It is noteworthy that the compounds did not interfere with the RNA immobilized on the SPR chip (Fig. 2E).

The data presented here show that our SPR approach allows efficient screening of anti-RdRp compounds. Our results confirm that suramin is a potent inhibitor of RdRp binding to RNA, thus a promising drug for the treatment of SARS-CoV-2 infection to help in this tiring battle with the virus.

#### Author contributions

Conceptualization, MM, GB, MB, Methodology, MM, GB, MB, Investigation, MM, GB, Resources, MB, Writing – Original Draft, MM, MB, Writing Review & Editing, MM, GB, MB, Supervision, GB, MB, Funding Acquisition, MB.

#### Declaration of Competing Interest

The authors declare that they have no known competing financial interests or personal relationships that could have appeared to influence the work reported in this paper.

#### Acknowledgments

We thank Uroš Petrovič for his help in obtaining the RdRp protein. This work was funded by grants to MM and MB from the Slovenian Research Agency (P1-0207 and J4-1778). The SPR measurements were performed at the Infrastructural centre for molecular interactions analysis at the Department of Biology, University of Ljubljana.

#### References

- Abdelnabi, R., de Moraes, A.T.S., Leyssen, P., Imbert, I., Beaucourt, S., Blanc, H., Froeyen, M., Vignuzzi, M., Canard, B., Neyts, J., Delang, L., 2017. Understanding the mechanism of the broad-spectrum antiviral activity of favipiravir (T-705): key role of the F1 motif of the viral polymerase. *J. Virol.* 91, e00487–17. <https://doi.org/10.1128/jvi.00487-17>.
- Agostini, M.L., Andres, E.L., Sims, A.C., Graham, R.L., Sheahan, T.P., Lu, X., Smith, E.C., Case, J.B., Feng, J.Y., Jordan, R., Ray, A.S., Cihlar, T., Siegel, D., Mackman, R.L., Clarke, M.O., Baric, R.S., Denison, M.R., 2018. Coronavirus susceptibility to the antiviral remdesivir (GS-5734) is mediated by the viral polymerase and the proofreading exoribonuclease. *MBio* 9. <https://doi.org/10.1128/mBio.00221-18> e00221–e00218.
- Ahn, D.G., Choi, J.K., Taylor, D.R., Oh, J.W., 2012. Biochemical characterization of a recombinant SARS coronavirus nsp12 RNA-dependent RNA polymerase capable of copying viral RNA templates. *Arch. Virol.* 157, 2095–2104. <https://doi.org/10.1007/s00705-012-1404-x>.
- Chien, M., Anderson, T.K., Jockusch, S., Tao, C., Li, X., Kumar, S., Russo, J.J., Kirchdoerfer, R.N., Ju, J., 2020. Nucleotide analogues as inhibitors of SARS-CoV-2 polymerase, a key drug target for Covid-19. *J. Proteome Res.* 19, 4690–4697. <https://doi.org/10.1021/acs.jproteome.0c00392>.
- Elfiky, A.A., 2020. Anti-HCV, nucleotide inhibitors, repurposing against Covid-19. *Life Sci.* 248, 117477 <https://doi.org/10.1016/j.lfs.2020.117477>.
- Fornelos, N., Butala, M., Hodnik, V., Anderlüh, G., Bamford, J.K., Salas, M., 2015. Bacteriophage GIL01 gp7 interacts with host LexA repressor to enhance DNA binding and inhibit RecA-mediated auto-cleavage. *Nucleic Acids Res.* 43, 7315–7329. <https://doi.org/10.1093/nar/gkv634>.
- Furuta, Y., Takahashi, K., Kuno-Maekawa, M., Sangawa, H., Uehara, S., Kozaki, K., Nomura, N., Egawa, H., Shiraki, K., 2005. Mechanism of action of T-705 against influenza virus. *Antimicrob. Agents Chemother.* 49, 981–986. <https://doi.org/10.1128/AAC.49.3.981-986.2005>.
- Gordon, C.J., Tchesnokov, E.P., Feng, J.Y., Porter, D.P., Götte, M., 2020. The antiviral compound remdesivir potently inhibits RNA-dependent RNA polymerase from Middle East respiratory syndrome coronavirus. *J. Biol. Chem.* 295, 4773–4779. <https://doi.org/10.1074/jbc.AC120.013056>.
- Hillen, H.S., Kocic, G., Farnung, L., Dienemann, C., Tegunov, D., Cramer, P., 2020. Structure of replicating SARS-CoV-2 polymerase. *Nature* 584, 154–156. <https://doi.org/10.1038/s41586-020-2368-8>.
- Jácome, R., Campillo-Balderas, J.A., Ponce de León, S., Becerra, A., Lazcano, A., 2020. Sofosbuvir as a potential alternative to treat the SARS-CoV-2 epidemic. *Sci. Rep.* 10, 1–5. <https://doi.org/10.1038/s41598-020-66440-9>.
- Jockusch, S., Tao, C., Li, X., Chien, M., Kumar, S., Morozova, I., Kalachikov, S., Russo, J. J., Ju, J., 2020. Sofosbuvir terminated RNA is more resistant to SARS-CoV-2 proofreader than RNA terminated by remdesivir. *Sci. Rep.* 10, 16577. <https://doi.org/10.1038/s41598-020-73641-9>.
- Ju, J., Li, X., Kumar, S., Jockusch, S., Chien, M., Tao, C., Morozova, I., Kalachikov, S., Kirchdoerfer, R.N., Russo, J.J., 2020. Nucleotide analogues as inhibitors of SARS-CoV polymerase. *Pharmacol. Res. Perspect.* 8, e00674 <https://doi.org/10.1002/prp2.674>.
- Kocic, G., Hillen, H.S., Tegunov, D., Dienemann, C., Seitz, F., Schmitzova, J., Farnung, L., Stewert, A., Höbartner, C., Cramer, P., 2021. Mechanism of SARS-CoV-2 polymerase stalling by remdesivir. *Nat. Commun.* 12, 279. <https://doi.org/10.1038/s41467-020-20542-0>.
- Öberg, B., 2006. Rational design of polymerase inhibitors as antiviral drugs. *Antiviral Res.* 71, 90–95. <https://doi.org/10.1016/j.antiviral.2006.05.012>.
- Reznik, S.E., Ashby, C.R., 2017. Sofosbuvir: an antiviral drug with potential efficacy against Zika infection. *Int. J. Infect. Dis.* 55, 29–30. <https://doi.org/10.1016/j.ijid.2016.12.011>.
- Salgado-Benvindo, C., Thaler, M., Tas, A., Ogando, N.S., Bredenbeek, P.J., Ninaber, D.K., Wang, Y., Hiemstra, P.S., Snijder, E.J., Van Hemert, M.J., 2020. Suramin inhibits SARS-CoV-2 infection in cell culture by interfering with early steps of the replication cycle. *Antimicrob. Agents Chemother.* 64, 1–11. <https://doi.org/10.1128/AAC.00900-20>.
- Shi, F., Xie, Y., Shi, L., Xu, W., 2013. Viral RNA polymerase: a promising antiviral target for influenza A virus. *Curr. Med. Chem.* 20, 3923–3934. <https://doi.org/10.2174/09298673113209990208>.
- Subissi, L., Posthuma, C.C., Collet, A., Zevenhoven-Dobbe, J.C., Gorbalenya, A.E., Decroly, E., Snijder, E.J., Canard, B., Imbert, I., 2014. One severe acute respiratory syndrome coronavirus protein complex integrates processive RNA polymerase and exonuclease activities. *Proc. Natl. Acad. Sci. U. S. A.* 111, e3900–e3909. <https://doi.org/10.1073/pnas.1323705111>.
- Tchesnokov, E.P., Feng, J.Y., Porter, D.P., Götte, M., 2019. Mechanism of inhibition of ebola virus RNA-dependent RNA polymerase by remdesivir. *Viruses* 11, 1–16. <https://doi.org/10.3390/v11040326>.
- Wiedemar, N., Hauser, D.A., Mäser, P., 2020. 100 years of suramin. *Antimicrob. Agents Chemother.* 64, e01168–19. <https://doi.org/10.1128/AAC.01168-19>.
- Wu, F., Zhao, S., Yu, B., Chen, Y.M., Wang, W., Song, Z.G., Hu, Y., Tao, Z.W., Tian, J.H., Pei, Y.Y., Yuan, M.L., Zhang, Y.L., Dai, F.H., Liu, Y., Wang, Q.M., Zheng, J.J., Xu, L., Holmes, E.C., Zhang, Y.Z., 2020. A new coronavirus associated with human respiratory disease in China. *Nature* 579, 265–269. <https://doi.org/10.1038/s41586-020-2008-3>.
- Yin, W., Luan, X., Li, Z., Zhou, Z., Wang, Qingxing, Gao, M., Wang, X., Zhou, F., Shi, J., You, E., Liu, M., Wang, Qingxia, Jiang, Y., Jiang, H., Xiao, G., Zhang, L., Yu, X., Zhang, S., Eric Xu, H., 2021. Structural basis for inhibition of the SARS-CoV-2 RNA

- polymerase by suramin. *Nat. Struct. Mol. Biol.* 28, 319–325. <https://doi.org/10.1038/s41594-021-00570-0>.
- Zhai, Y., Sun, F., Li, X., Pang, H., Xu, X., Bartlam, M., Rao, Z., 2005. Insights into SARS-CoV transcription and replication from the structure of the nsp7-nsp8 hexadecamer. *Nat. Struct. Mol. Biol.* 12, 980–986. <https://doi.org/10.1038/nsmb999>.
- Ziebuhr, J., 2005. The coronavirus replicase. In: Enjuanes, L. (Ed.), *Coronavirus Replication and Reverse Genetics*, Current Topics in Microbiology and Immunology. Springer, Berlin, Heidelberg, pp. 57–94. [https://doi.org/10.1007/3-540-26765-4\\_3](https://doi.org/10.1007/3-540-26765-4_3).